Supporting information

Multiple CO_2 reduction mediated by heteronuclear metal carbide cluster anions $RhTaC_2^-$

Xing-Yue He[a,#], Yun-Zhu Liu[b,c,d,#], Si-Dun Wang[e], Xing-Wang Lan[a,*], Xiao-Na Li[b,d,*], Sheng-Gui He[b,c,d]

[a] *Key Laboratory of Chemical Biology of Hebei Province, College of Chemistry and Environmental Science, Hebei University, Baoding, Hebei,071002, P.R. China*

[b] *State Key Laboratory for Structural Chemistry of Unstable and Stable Species, Institute of Chemistry, Chinese Academy of Sciences, Beijing 100190, China*

[c] *University of Chinese Academy of Sciences, Beijing 100049, P. R. China*

[d] *Beijing National Laboratory for Molecular Sciences and CAS Research/Education Center of Excellence in Molecular Sciences, Beijing 100190, China*

[e] *School of Chemistry and Chemical Engineering, South China University of Technology, 381 Wushan Road, Tianhe District, Guangzhou 510641, China*

[#] *The two authors contribute equally.*

Corresponding authors. hxlxw@sina.cn (X. W. Lan); lxn@iccas.ac.cn (X. N. Li)

Additional experimental results

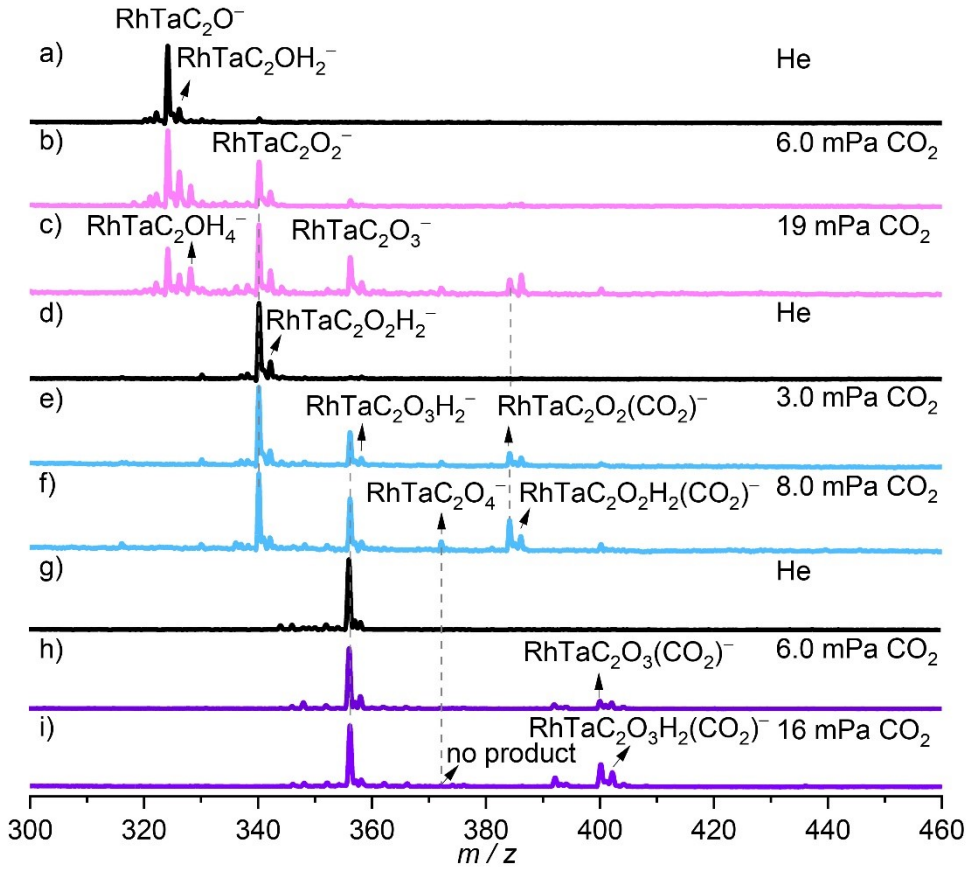

Fig. S1. Time-of-flight mass spectra for the reactions of mass-selected $RhTaC_2O^-$ (a–c), $RhTaC_2O_2^-$ (d–f) and $RhTaC_2O_3^-$ (g–i) with CO_2. The time period for the reactions of $RhTaC_2O^-$, $RhTaC_2O_2^-$ and $RhTaCO_3^-$ with CO_2 is about 1.7 ms, 1.7 ms, and 3.8 ms, respectively. The reactant gas pressures are shown in mPa (= 10^{-3} Pa).

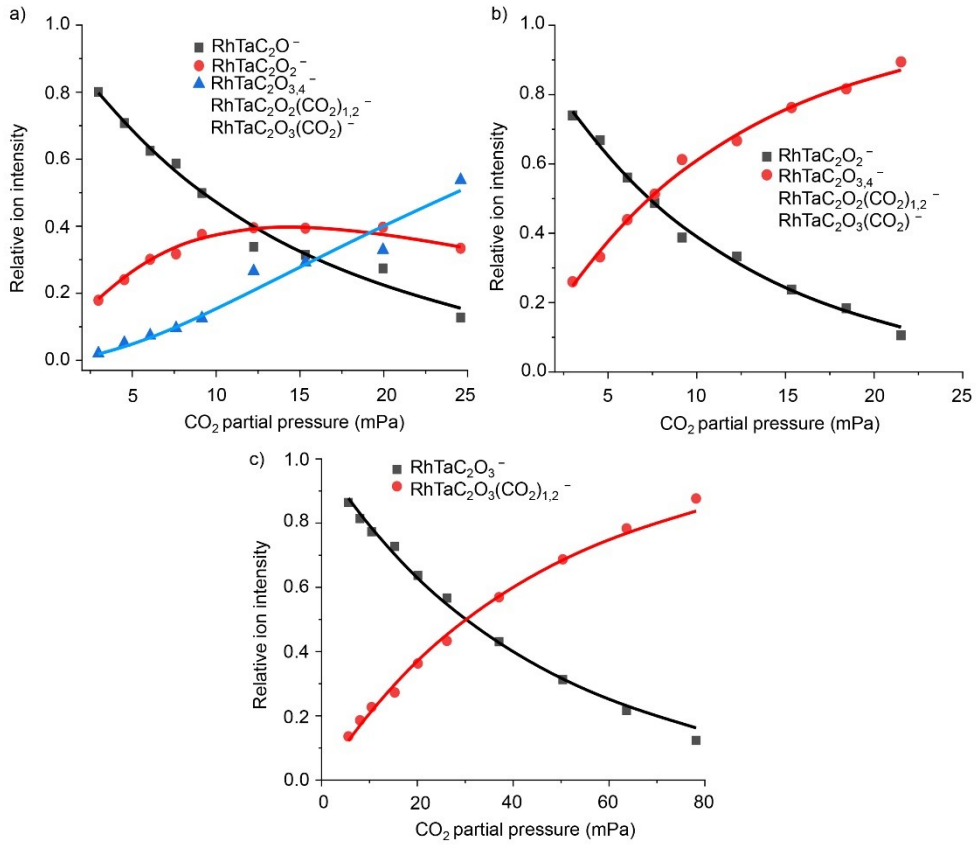

Fig. S2. Variations of ion intensities with respect to the CO_2 pressures on the reactions of products $RhTaC_2O^-$ (a), $RhTaC_2O_2^-$ (b), and $RhTaC_2O_3^-$ with CO_2 (c). The solid lines are fitted to the experimental data points by using the equations with the approximation of the pseudo-first-order reaction mechanism.

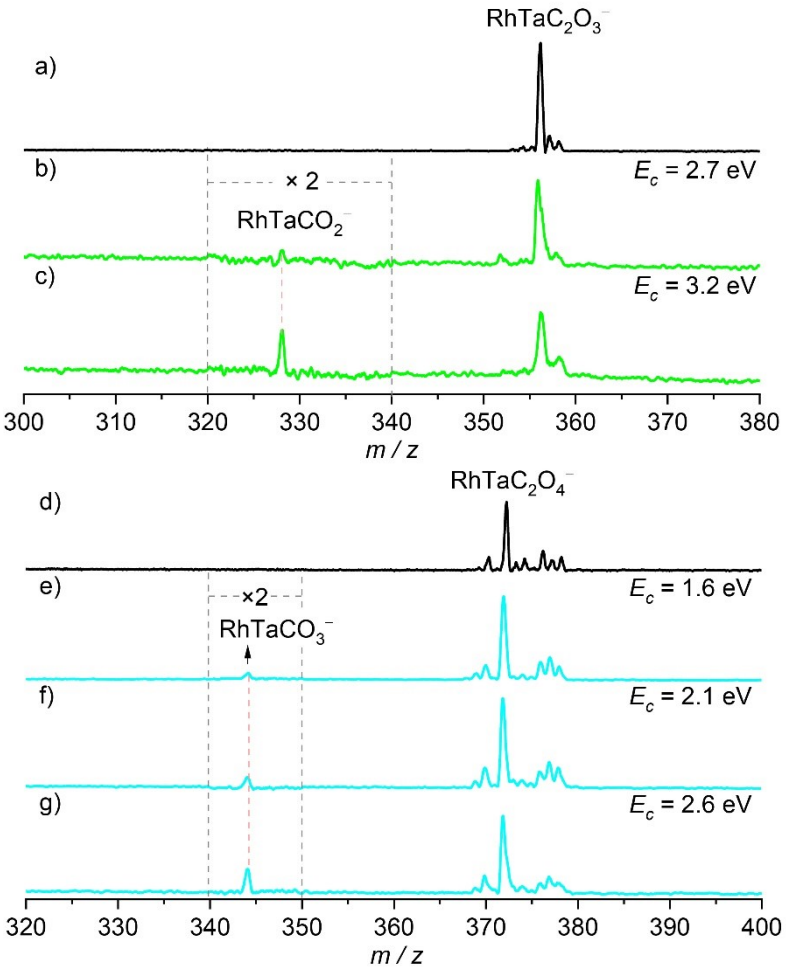

Fig. S3. Collision-induced dissociation (CID) spectra of mass-selected $RhTaC_2O_3^-$ and $RhTaC_2O_4^-$ clusters with 40 mPa Xe in the collision cell. The center-of-mass collision energy (E_c) is given.

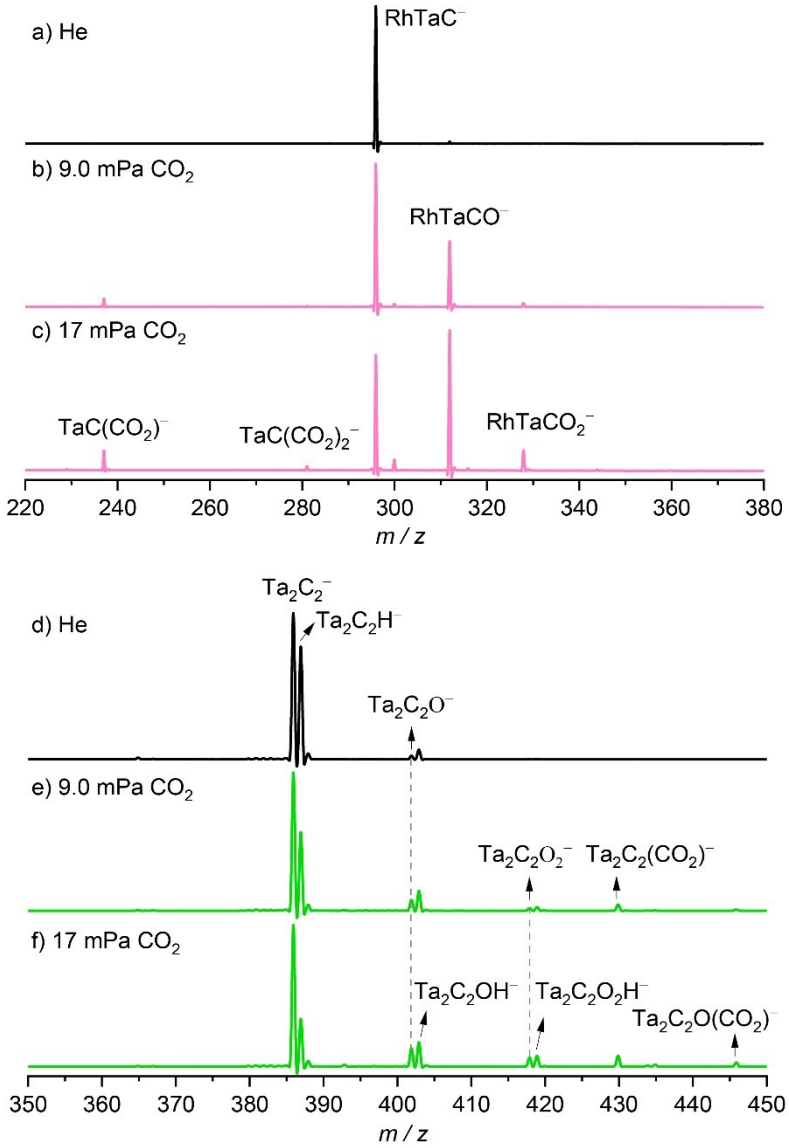

Fig. S4. Time-of-flight mass spectra for the reactions of mass-selected $RhTaC^-$ (b,c) and $Ta_2C_2^-$ (e,f) with CO_2. The reaction time for both reactions is about 1.7 ms. The reactant gas pressures are shown in mPa (= 10^{-3} Pa).

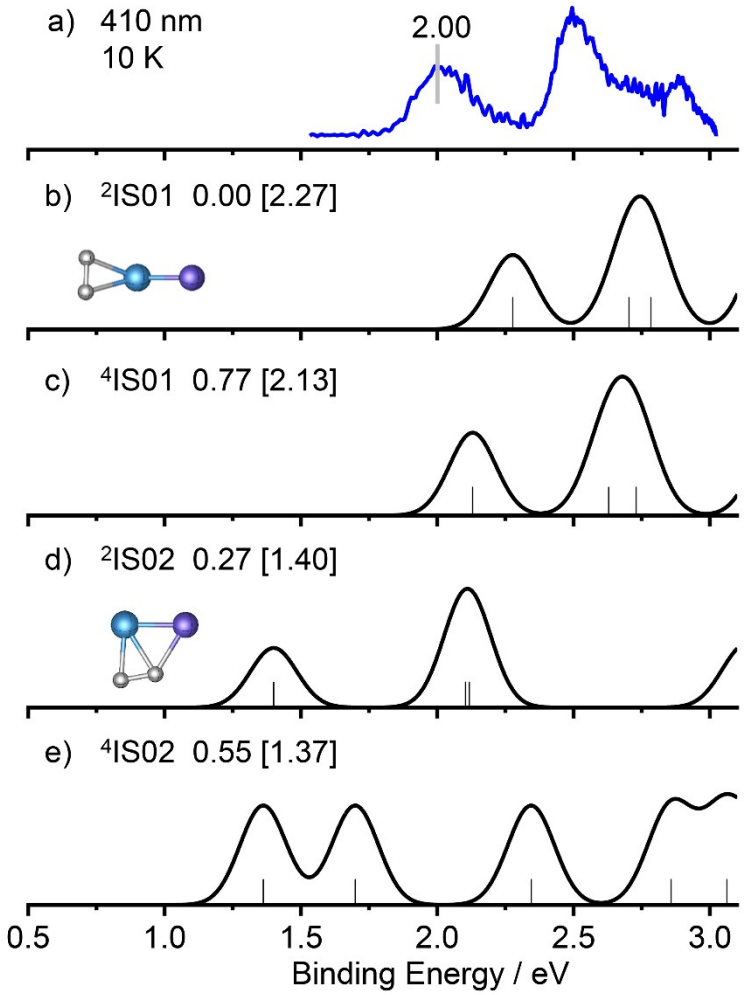

Fig. S5. The photoelectron spectrum of $RhTaC_2^-$ measured with 410 nm at 10 K (a) and the simulated density of state spectra for the low-lying $RhTaC_2^-$ isomers (b-e) are shown. The relative energies of the $RhTaC_2^-$ isomers are given and more details can be found in Fig. S6. The superscripts represent the spin multiplicities. The vertical electron detachment energies (in the square brackets) in unit of eV are given.

Additional theoretical results

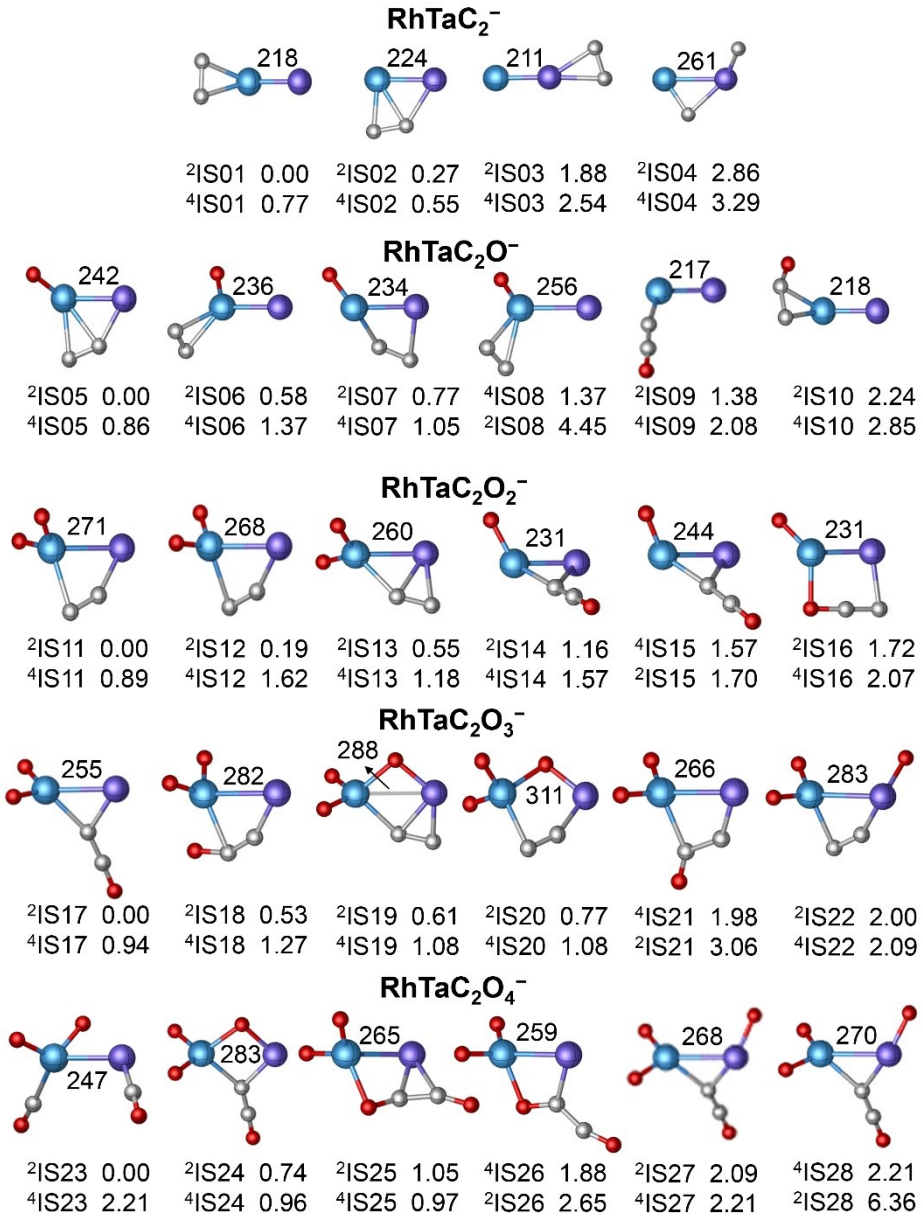

Fig. S6. Density functional theory (DFT) calculated isomers for $RhTaC_2O_n^-$ (n = 0–4) at the B3LYP level. The relative energies with respect to the lowest-lying isomer are given in eV. Bond lengths are given in pm. The superscripts represent the different spin multiplicities.

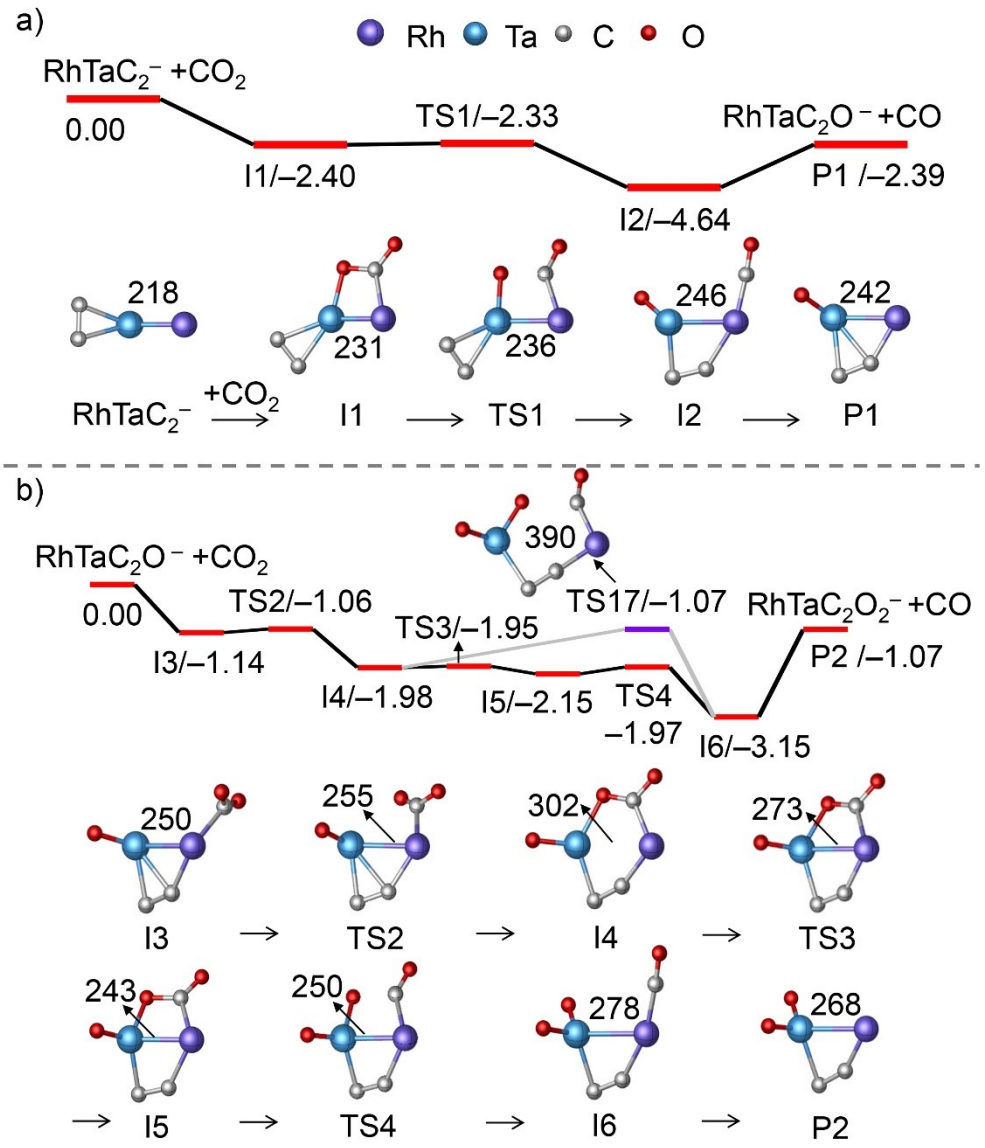

Fig. S7. The DFT-calculated potential energy profiles for the reactions $RhTaC_2^- + CO_2$ (a) $RhTaC_2O^- + CO_2$ (b) on the doublet state. The zero-point vibration corrected energies of intermediates (I*n*) and transition states (TS*n*) relative to the separate reactants are in units of eV. Bond lengths are given in pm.

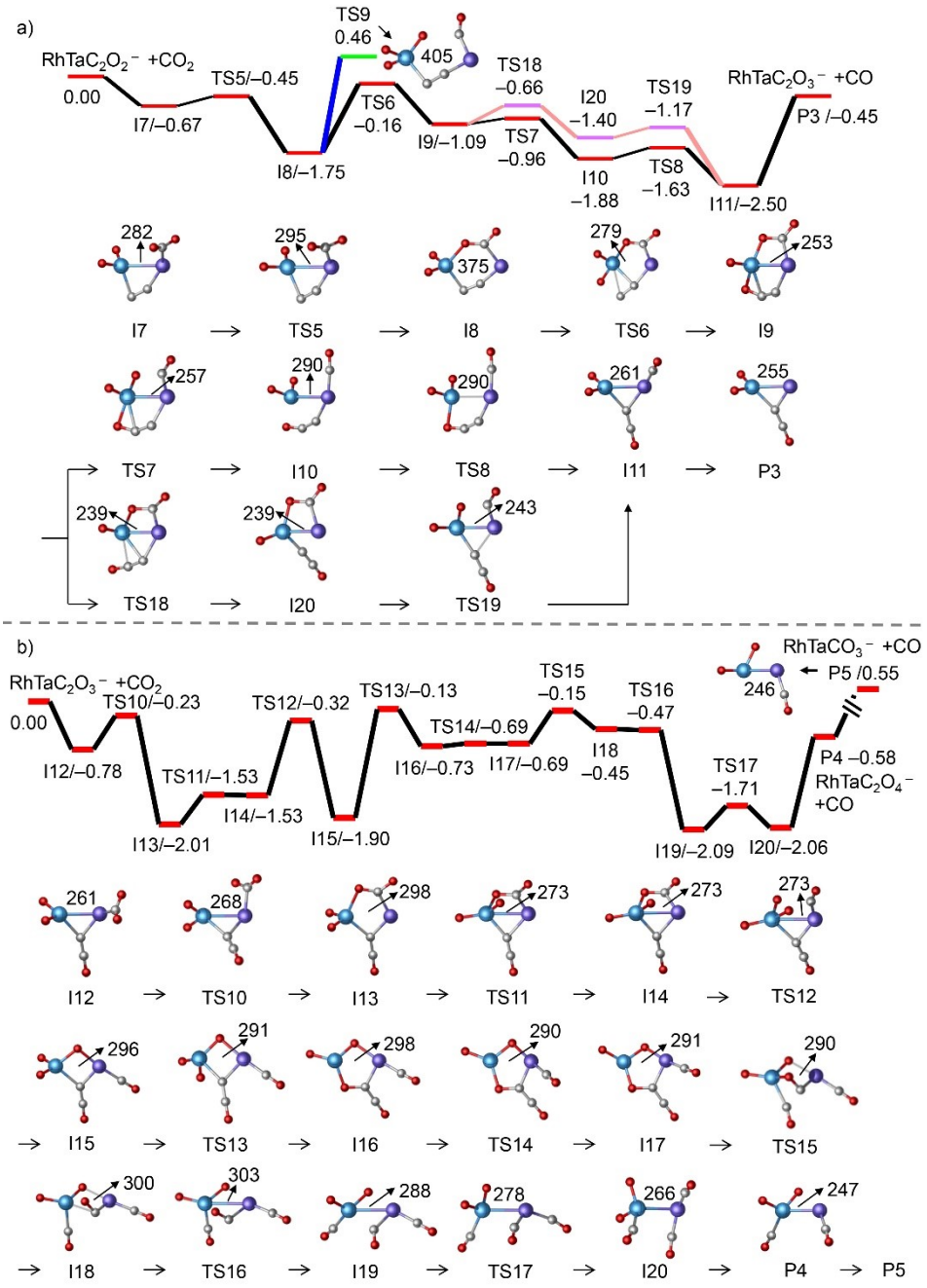

Fig. S8. The DFT-calculated potential energy profiles for the reactions $RhTaC_2O_2^-$ + CO_2 (a) $RhTaC_2O_3^-$ + CO_2 (b) on the doublet state. The zero-point vibration corrected energies of I*n* and TS*n* relative to the separate reactants are in units of eV. Bond lengths are given in pm.

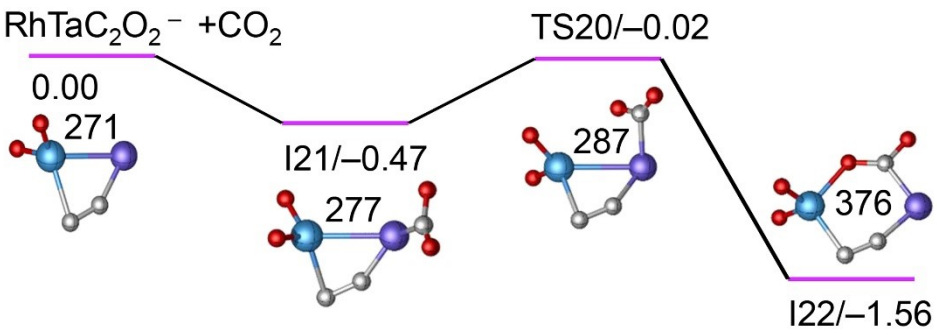

Fig. S9. The DFT-calculated potential energy profile for the reaction of the lowest-lying $RhTaC_2O_2^-$ isomer (IS11) with CO_2 on the doublet state. The zero-point vibration corrected energies of I*n* and TS*n* relative to the separate reactants are in units of eV. Bond lengths are given in pm.

Table. S1. Experimental and calculated bond dissociation enthalpies (in eV).

	Rh–Ta	**Rh–C**	**Rh–O**	**Ta–C**	**Ta–O**	**C–O**
EXP.	~	5.97	4.16	~	8.66	11.12
B3LYP	**3.78**	**5.30**	**3.80**	**4.94**	**7.91**	**10.80**
M06L	4.73	6.06	4.35	5.34	8.06	10.93
BPW91	5.07	6.31	4.64	5.50	8.46	11.19
BLYP	4.75	6.18	4.66	5.27	8.31	11.12
BP86	5.24	6.49	4.81	5.70	8.64	11.37
TPSS	5.11	6.22	4.59	5.34	8.24	10.78
PBEPBE	5.27	6.56	4.87	5.78	8.66	11.43
BPBE	5.10	6.34	4.65	5.53	8.48	11.20

Table S2. The estimated rate constants (in unit of s^{-1}) of internal conversion (k_{int}) and CO desorption (k_d) for reactions $RhTaC_2O_{0\text{-}3}^- + CO_2$ based on the RRKM and VTST theories.

Reactions	k_d	k_{int}
$RhTaC_2^- + CO_2$	4.8×10^{11}	-
$RhTaC_2O^- + CO_2$	3.0×10^{9}	-
$RhTaC_2O_2^- + CO_2$	1.5×10^{6}	6.9×10^{2} (I8 → TS6)
$RhTaC_2O_3^- + CO_2$	1.1×10^{8}	5.4×10^{1} (I15 → TS13)